Dynamic and modular formation of a synergistic transphosphorylation catalyst

Dynamic and modular formation of a synergistic transphosphorylation catalyst

Chloe Z.-J. Ren[1,2], Pablo Solís-Muñana[1,2], Gregory G. Warr[4], Jack L.-Y. Chen*[,1,2,3]

[1] Centre for Biomedical and Chemical Sciences, School of Science, Auckland University of Technology, Auckland 1010, New Zealand

[2] The MacDiarmid Institute for Advanced Materials and Nanotechnology, Victoria University of Wellington, Wellington 6140, New Zealand

[3] Department of Biotechnology, Chemistry and Pharmaceutical Sciences, Università degli Studi di Siena, 53100 Siena, Italy

[4] School of Chemistry, The University of Sydney, Sydney, NSW 2006, Australia

KEYWORDS cooperative catalysis, self-assembly, biomimetic catalysis, synergistic catalysis, multifunctional catalysis

ABSTRACT: Enzymes accelerate chemical reactions by forming cooperative interactions using precisely positioned functional groups. This has inspired the construction of artificial catalysts by the attachment of functional groups onto molecular scaffolds or solid supports to induce synergistic interactions. Herein, the transphosphorylation reaction is used as a model to demonstrate that cooperativity can also occur intermolecularly between multiple functional groups within self-assembled vesicular structures. We demonstrate that the modular and dynamic nature of such systems allow for triggered reorganization, and the up- or down-regulation of catalytic activity. Such concepts have potential to be used in the design of synergistic catalysts and their incorporation into responsive catalytic systems in water.

Cooperative interactions between precisely positioned functional groups in an active site are one of the hallmarks of natural enzymes.[1] The simultaneous activation of a reactant by proximal functional groups decreases the energy of a transition state to a much greater degree than the sum of each functional group acting independently. Taking this queue from biological systems, chemists have devised numerous strategies for the pre-organization of functional groups to allow the formation of multiple contacts with a bound substrate.[2] Examples include the covalent attachment of functional groups onto molecular scaffolds,[3] within polymers,[4] and the immobilization of functional groups onto dendrimers[5] or nanoparticles.[6] The majority of these studies are based on the idea that an enzyme acts as an "entropy trap", where rate acceleration is achieved by the precise positioning of catalytic units and the restriction of rotation of a substrate within the catalytic site.[1b] However, as few supramolecular catalysts have progressed to become synthetically useful, it has been suggested that "the fear of entropy has taken supramolecular chemists too far in the direction of rigidity and preorganization."[1b] Moreover, it is now generally accepted that enzymes are highly dynamic and conformationally diverse structures that flex and mold in response to the chemical environment.[1a,7]

This inspired us to examine the use of hydrophobic interactions to induce the formation of cooperative catalysts in an intermolecular fashion.[8] Work by the groups of Ulijn, Das and others show how reversible cooperativity within assembled systems can be utilized to exhibit switchable or transient catalysis by controlling the self-assembly process.[9] In these systems, the advantage of utilizing dynamic assembly versus covalently-linked scaffolds is clearly evident, offering the potential to create artificial systems with life-like characteristics.[10,11]

We recently demonstrated an artificial system where the substrate of a chemical reaction induced the formation of a catalyst from inactive precursors.[8,12] The precursor employed was amphiphilic **C$_{16}$TACN**·Zn^{2+} (**1**·Zn^{2+}), which terminated with a Zn^{2+}-complexed 1,4,7-triazacyclononane (**TACN**) head group (Figure 1). Systems featuring the **TACN**·Zn^{2+} moiety have been shown to efficiently catalyze the transphosphorylation of 2-hydroxypropyl-4-nitrophenol phosphate (**HPNPP**),

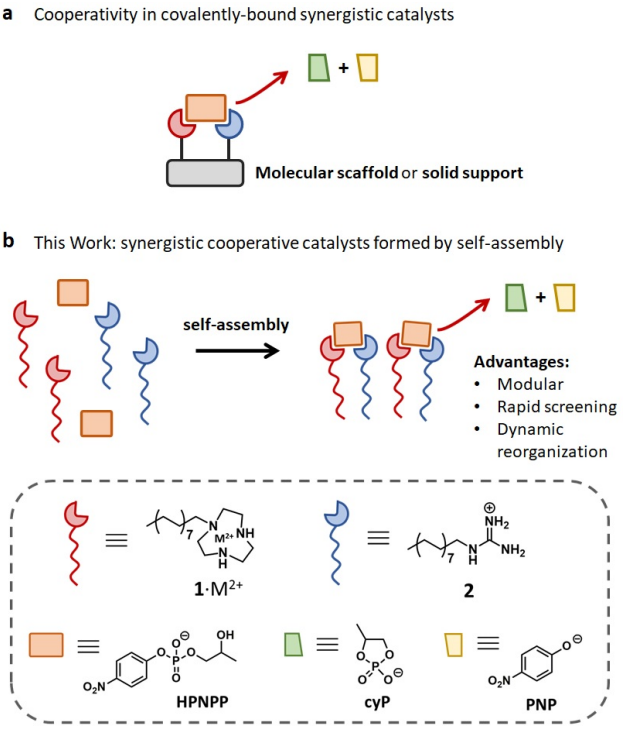

Figure 1. General representations of a) a cooperative catalyst formed by covalent linkage onto a molecular scaffold or a solid support and b) a multi-component cooperative catalyst formed by self-assembly. The modular nature of the self-assembled catalyst system enables rapid screening of pre-catalyst ratios. The dynamic nature allows for *in situ* modulation of catalytic rates. M^{2+} = Zn^{2+} or Cu^{2+}.

which is a model substrate for RNA hydrolysis.[13] Importantly, this transphosphorylation reaction is known to require two metal ions acting cooperatively to achieve efficient reactivity.[14] In our studies, we observed that the introduction of substrate **HPNPP** into the reaction medium induced the self-assembly of **1**·Zn^{2+} amphiphiles into vesicular assemblies. The negatively charged phosphate of **HPNPP** interacts strongly with the headgroup of the amphiphile, significantly decreasing the critical assembly concentration (CAC) of **1**·Zn^{2+} in solution. Importantly, **TACN**·Zn^{2+} units in the non-assembled form are not catalytically active and the formation of vesicular structures was essential for the **TACN**·Zn^{2+} headgroups to form catalytic pockets.[15] Herein, we demonstrate that such self-assembled systems are amenable to the formation of multicomponent synergistic catalysts. The modularity of these systems allows for the rapid screening of catalyst ratios, where varying degrees of synergism are observed. Their dynamic nature also permits the *in situ* reorganization of one catalyst system into another, allowing for the up- and down-regulation of catalytic activity.

With the aim of incorporating additional functional groups into our catalytic system containing **1**·Zn^{2+}, we examined the literature and were inspired by reports of artificial phosphodiesterases that featured guanidinium units acting cooperatively.[6c,16] The guanidinium group, present in many enzyme active sites as the amino acid arginine, is known to interact strongly with phosphates via a two-point hydrogen bonding motif.[17] Artificial phosphodiesterases have also been synthesized that exhibit cooperativity between guanidinium units and metal-bound ligands.[18] The guanidinium unit is believed to

Scheme 1. Synthesis of the amphiphile C_{16}-guanidinium **2** and the control molecule C_4-guanidinium **6**.

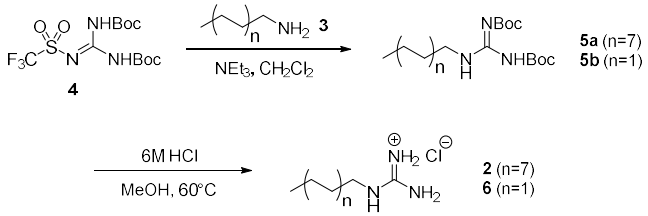

complement the catalytic activity of the metal ions by aiding with substrate binding and activation, as well as transition state stabilization.[16b] Existing examples feature guanidinium and metal-binding units linked together covalently to reinforce their ability to act cooperatively. As an example, Salvio and co-workers reported the attachment of guanidinium units and **TACN** onto the upper ring of *cone*-calix[4]arenes to generate hetero-bifunctional catalysts.[18a,d]

We started by investigating the ability of amphiphiles containing a guanidinium headgroup to form vesicular assemblies in the presence of **HPNPP**. C_{16}-guanidinium **2** was synthesized using a sequence adapted from a procedure reported by Salvio *et al*.[18d] The route began with the coupling of hexadecylamine (**3**) with an electrophilic source of guanidine (1,3-di-Boc-2-(trifluoromethylsulfonyl)guanidine **4**), to form guanidine **5a** (Scheme 1). Removal of the Boc protecting groups using hydrochloric acid afforded the desired amphiphilic pre-catalyst **2**, containing a C_{16}-chain. An analogous guanidinium-based pre-catalyst (**6**) with a C_4-alkyl chain was also

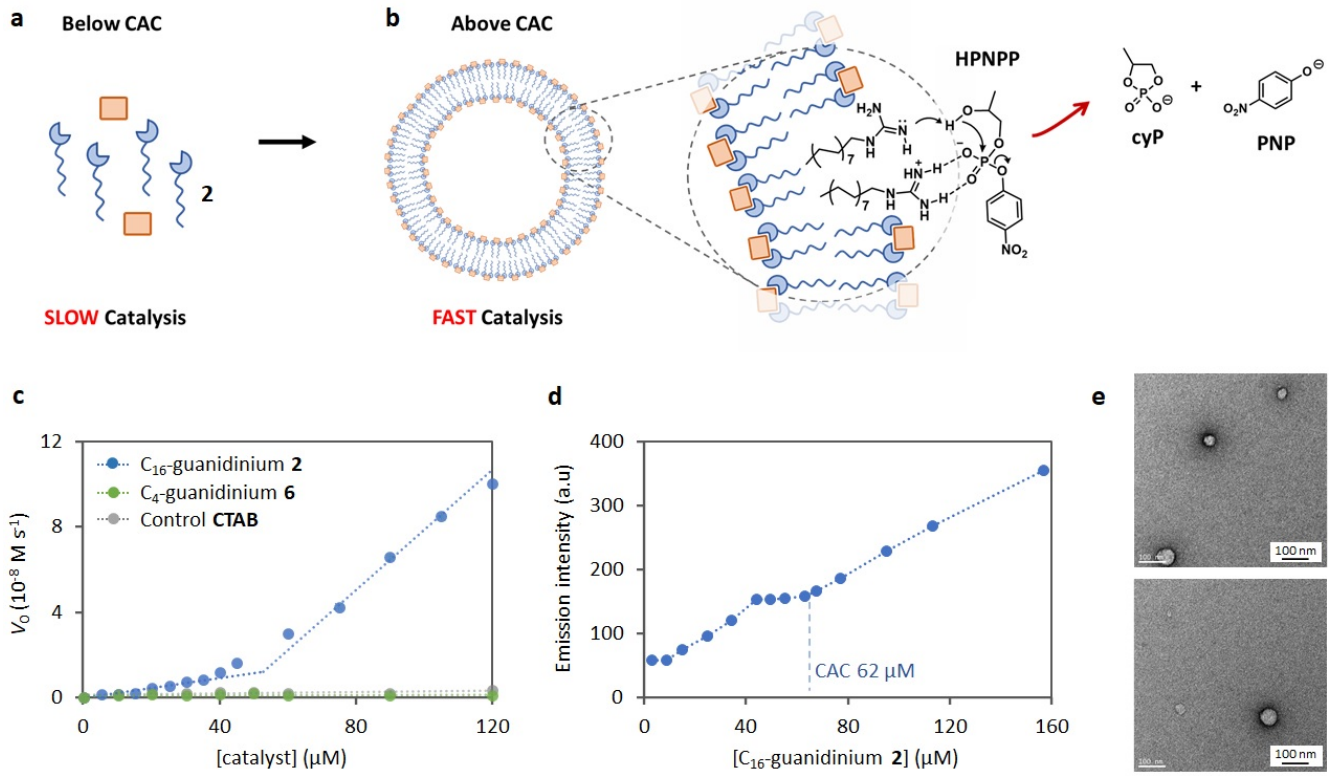

Figure 2. Examining the ability of C_{16}-guanidinium **2** to act as a cooperative catalyst for phosphodiesterase activity. a) C_{16}-guanidinium **2** in a non-assembled state; b) self-assembly of C_{16}-guanidinium **2** into vesicular structures, aided by binding to the **HPNPP** substrate, which decreases the CAC; c) initial rates of **HPNPP** hydrolysis at increasing concentrations of C_{16}-guanidinium **2**, C_4-guanidinium **6** and CTAB, aqueous buffer pH = 9.1 ([CHES] = 5 mM), [**HPNPP**] = 500 μM, 40 °C); d) emission intensity profiles for Nile red (2 μM, λ_{ex} = 570 nm, λ_{em} = 635 nm) at increasing C_{16}-guanidinium **2** concentrations; e) representative TEM images of C_{16}-guanidinium **2** (70 μM) in aqueous buffer pH = 9.1 ([CHES] = 5 mM), [**HPNPP**] = 500 μM.

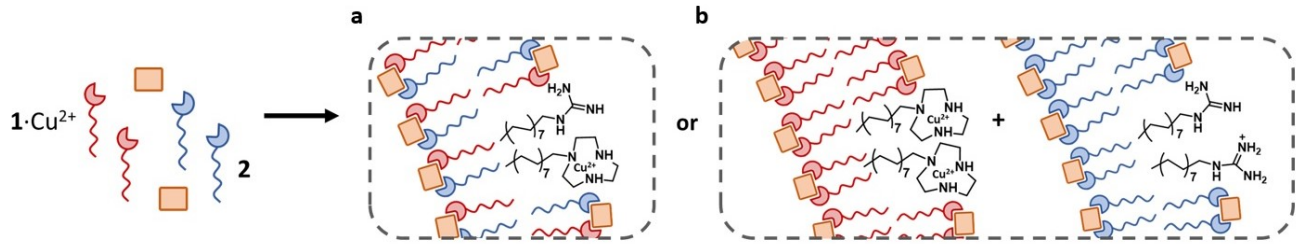

Figure 3. Representation of **C16TACN**·Cu^{2+} (**1**·Cu^{2+}, red) and C_{16}-guanidinium **2** (blue) a) mixing to form heterogeneous vesicular assemblies and b) self-sorting to form homogenous vesicular assemblies consisting of only **1**·Cu^{2+} and only C_{16}-guanidinium **2**.

synthesized to act as a control molecule for subsequent experiments. The ability of C_{16}-guanidinium **2** to act as a catalyst for the cleavage of the phosphodiester bond (Figure 2b) was first investigated in a number of different pH's in aqueous buffer (see Supporting Information, S4a for details). With **HPNPP** as the substrate, the transphosphorylation reaction results in the formation of a cyclic phosphate (**cP**) and the release of *p*-nitrophenolate (**PNP**), which allows the reaction to be determined spectrophotometrically by measuring the absorbance at 410 nm (Figure 2b). Figure 2c shows a plot of the initial rates of reaction with increasing concentrations of C_{16}-guanidinium **2** (0 – 120 μM) at pH 9.1 ([CHES] = 5 mM) and **HPNPP** (500 μM). The transphosphorylation rate can be observed to slowly increase at amphiphile concentrations up to 40 μM, with the reaction rate rapidly increasing above 60 μM of C_{16}-guanidinium **2**. The observed change in slope occurs at ~55 μM, which closely matched the CAC (62 μM) as determined by fluorescence titration with Nile red, suggesting that structure formation is important for catalytic activity (Figure 2d, see Supporting Information, S4b for details). The presence of assembled structures was confirmed by dynamic light scattering (DLS) measurements (in the presence of a model substrate that is not cleaved) and observed to have an average hydrodynamic diameter of ~100 nm (Figure S2). These structures were also visualized using transmission electron microscopy (TEM), which supported the presence of vesicular assemblies (Figure 2e). It is important to note that the presence of **HPNPP** induces the self-assembly of C_{16}-guanidinium **2** into vesicular structures, effectively forming the catalyst that causes its own degradation. This is evidenced by a decrease in the CAC of C_{16}-guanidinium **2** at increasing **HPNPP** concentrations (Figure S5).

To demonstrate that self-assembly is required for catalysis, the catalytic activity of C_4-guanidinium **6**, containing a shorter alkyl chain, was also measured (Figure 2c, green circles). Low catalytic activity was observed with amphiphile **6** which is likely due to the inability to form vesicular structures under the conditions examined. To demonstrate that catalytic activity was not simply due to local changes in pH induced by high local concentrations of positive ions, the rate of **HPNPP** cleavage was also measured at increasing concentrations of the cationic amphiphile cetyltrimethylammonium bromide (CTAB, Figure 2c, grey circles). Low catalytic activity was observed in the presence of CTAB, comparable to the rates observed with control amphiphile **6**.

In this and our previous examples,[8] only a single pre-catalytic unit was used for the assembly of the catalytic system. In an attempt to generate a multi-component catalyst, we proceeded to mix **C16TACN**·Cu^{2+} (**1**·Cu^{2+}) together with C_{16}-guanidinium **2**. The use of Cu^{2+} instead of Zn^{2+} as the metal ion was motivated by previous reports describing positive cooperation between **TACN**·Cu^{2+} and guanidinium units.[18g,h]

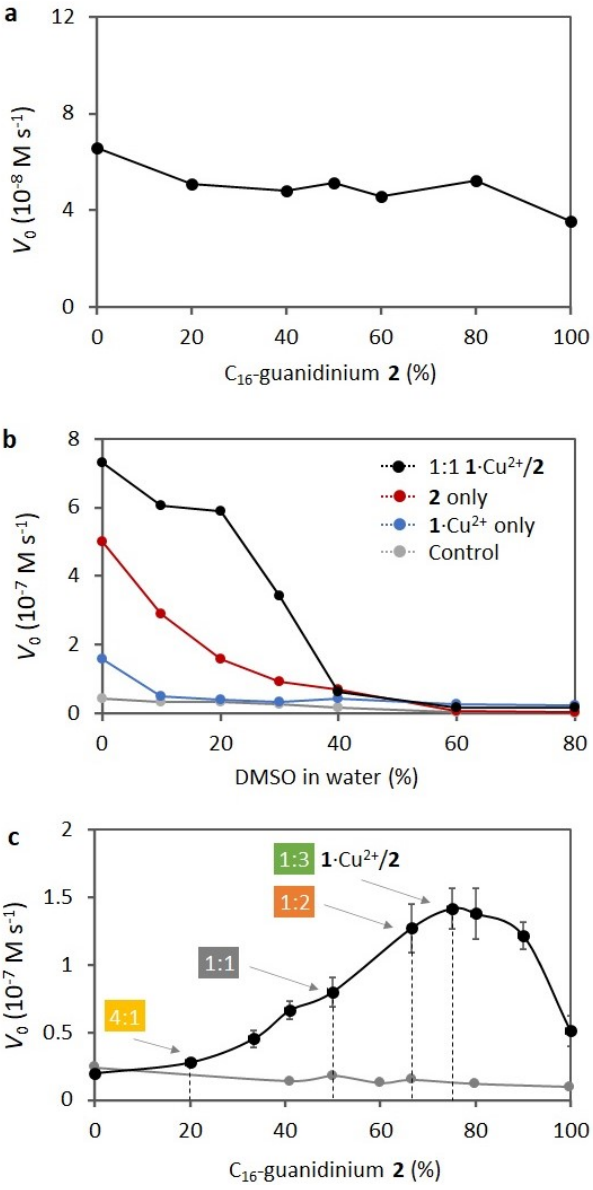

Figure 4. Examination of cooperativity between **1**·Cu^{2+} and C_{16}-guanidinium **2**. a) Initial rates of **HPNPP** cleavage at different proportions of **1**·Cu^{2+} to C_{16}-guanidinium **2**, [**1**·Cu^{2+}] + [**2**] = 200 μM, pH = 9.1 ([CHES] = 5 mM), [**HPNPP**] = 500 μM, 40 °C; b) initial rates of **HPNPP** cleavage in different DMSO/water solvent mixtures, [**1**·Cu^{2+}] = [**2**] = 100 μM, [NEt^iPr_2] = 1 mM), [**HPNPP**] = 500 μM, 40 °C, control is in the absence of catalyst; c) initial rates of **HPNPP** cleavage at different ratios of **1**·Cu^{2+} and C_{16}-guanidinium **2**, ([**1**·Cu^{2+}] + [**2**] = 200 μM, [NEt^iPr_2] = 1 mM, 20% DMSO in water), 20 °C. Control is using C_4-guanidinium **6** instead of C_{16}-guanidinium **2** (error bars depict the standard deviation).

However, the mixing of our two pre-catalysts is complicated by the uncertainty of whether heterogeneous assembly or self-sorted homogenous assembly of the amphiphiles would occur (Figure 3). We hoped to answer this question by measuring the catalytic activity of a mixture of the two amphiphiles in an attempt to detect any hint of synergism between the two functional groups – resulting in catalytic activity higher than each of the pre-catalysts on their own.

Figure 4a shows the catalytic activity of mixtures containing different ratios of **1**·Cu^{2+} and C_{16}-guanidinium **2** in aqueous buffer. The total concentration of catalysts in each experiment was maintained at 200 μM, which was well above the CAC of **1**·Cu^{2+} (20 μM) and C_{16}-guanidinium **2** (62 μM) under these conditions.[19] It can be seen from Figure 4a that the rate of reaction in the presence of only **1**·Cu^{2+} was 7.2×10^{-8} mol L^{-1} s^{-1} (far left), while the reaction rate with only C_{16}-guanidinium **2** was 4.0×10^{-8} mol L^{-1} s^{-1} (far right). The reaction rate at different proportions of **1**·Cu^{2+} to C_{16}-guanidinium **2** was observed to fall always between these two values, with no evidence of an enhancement in activity from the heterodimeric combination of these catalyst precursors. We therefore concluded that there was no evidence of cooperation between **1**·Cu^{2+} and C_{16}-guanidinium **2** under these conditions.

While initially disappointed, we were buoyed by studies which showed that binding interactions between guanidinium and phosphate groups could be increased in less aqueous solvent mixtures.[20] For this reason, the activity of several artificial phosphodiesterases have been examined in water/DMSO mixtures, which can also be used to simulate the less aqueous environment of an enzyme pocket.[18h,21] We therefore studied the catalytic activity of a 1:1 mixture of **1**·Cu^{2+}/C_{16}-guanidinium **2** in different water/DMSO solvent mixtures (Figure 4b). In mixtures of 80:20 and 60:40 DMSO:H_2O (v/v), the catalytic activity of 1:1 **1**·Cu^{2+}/**2** (black circles) was relatively low and approximately the sum of the catalytic activity of **1**·Cu^{2+} (blue circles) and C_{16}-guanidinium **2** (red circles) measured separately. However, at 30:70 DMSO:H_2O, the catalytic activity of 1:1 **1**·Cu^{2+}/**2** was significantly higher than the sum of the catalytic activity in the presence of only **1**·Cu^{2+} and only **2**, suggesting the presence of a synergistic effect between **1**·Cu^{2+} and **2**. This effect was even more pronounced at 20:80 DMSO:H_2O, with the catalytic activity of 1:1 **1**·Cu^{2+}/**2** 4.5 times faster than with only **2** and 15 times faster than with **1**·Cu^{2+} only. At low proportions of DMSO (10%), this synergistic effect is lower and in the absence of DMSO, the catalytic activity of 1:1 **1**·Cu^{2+}/**2** is approximately equal to the sum of the catalytic activities of **1**·Cu^{2} and **2** on their own. The modularity of this system allowed the facile examination of catalytic activity at different ratios of **1**·Cu^{2+} and C_{16}-guanidinium **2**. Subsequent experiments were performed in 20% DMSO/water, where the observed synergism between these two functional groups was the most pronounced. Taking 1:1 **1**·Cu^{2+}/**2** as a reference point, we found that increasing the ratio of **1**·Cu^{2+} to C_{16}-guanidium **2** resulted in a steady decrease in catalytic activity (Figure 4c), which reinforced the idea that cooperative interactions between **1**·Cu^{2+} and **2** is advantageous for catalysis. Interestingly, increasing the proportion of C_{16}-guanidinium **2** resulted in an increase in reaction rate, peaking at ~1:3 **1**·Cu^{2+}/**2**, before the reaction rate decreased at even higher proportions of **2**. Crucially, control experiments performed in the presence of **1**·Cu^{2+} and C_4-guanidinium **6** did not demonstrate this synergistic effect (Figure 4c, grey circles) and reinforces the notion that formation of vesicular structures and the resulting cooperativity is essential for catalytic activity.

These co-assembled systems were also examined using DLS and TEM to confirm that self-assembled structures were present in the less polar solvent mixture of 20% DMSO in water. Small angle neutron scattering (SANS) experiments were performed on the 1:3 **1**·Cu^{2+}/**2** system and the data obtained could be satisfactorily modelled as unilamellar vesicles with a bilayer thickness of 30 Å and a vesicle radius in the range 600-2000 Å (see SI, S4m for details).

To gain further insight into the catalytic systems generated at different ratios of **1**·Cu^{2+} to C_{16}-guanidinium **2**, the initial rates of reaction for three systems (1:1, 1:2 and 1:3 ratios of **1**·Cu^{2+}/**2**) were measured at increasing concentrations of **HPNPP** substrate (Figure 5a). Fitting of the saturation profiles to the Michaelis-Menten equation yielded a significantly lower K_M value of 1.3 ± 0.1 mM for the 1:3 **1**·Cu^{2+}/**2** system, which

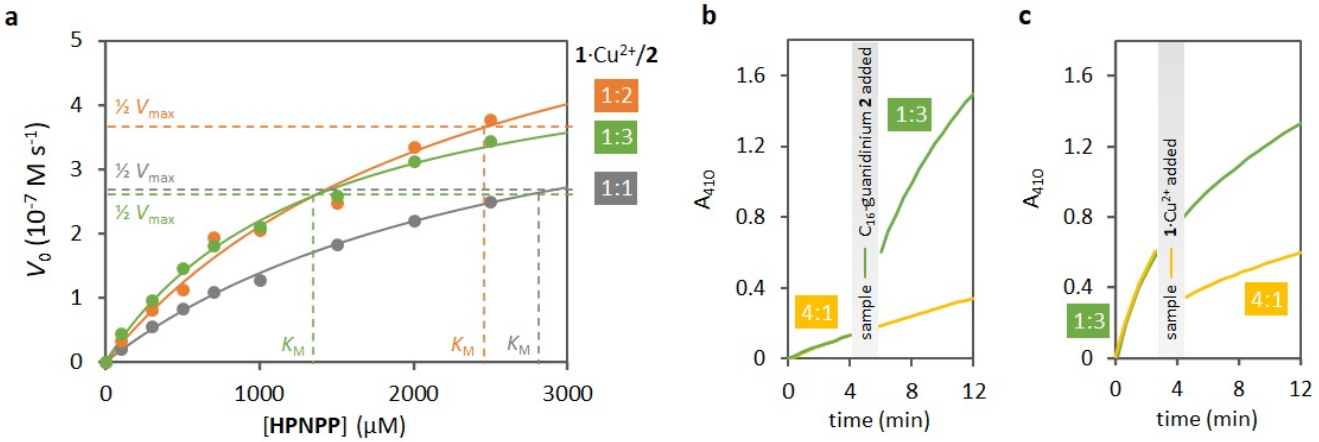

Figure 5. a) Examination of the catalytic efficiencies of three self-assembled systems, featuring 1:1, 1:2 and 1:3 ratios of **1**·Cu^{2+}/C_{16}-guanidinium **2**. The graph shows the initial rate of **HPNPP** cleavage at increasing **HPNPP** concentrations and fixed catalyst concentrations ([**1**·Cu^{2+}] + [**2**] = 200 μM, [NEt^iPr_2] = 1 mM), 20% DMSO in water). The solid lines are the data fits for a Michaelis-Menten mechanism. b) Demonstration of up-regulation. The graph shows absorbance as a function of time for a 4:1 **1**·Cu^{2+}/**2** system, to which at 4 min is added **2** to form a 1:3 **1**·Cu^{2+}/**2** system (green line). The yellow line follows the progress of a 4:1 system without the addition of **2**. c) Absorbance as a function of time for a 1:3 **1**·Cu^{2+}/**2** system, to which at 3 min is added **1**·Cu^{2+} to form a 4:1 **1**·Cu^{2+}/**2** system (yellow line). The green line follows the progress of a 1:3 system without the addition of **1**·Cu^{2+}.

suggests stronger binding interactions with the **HPNPP** substrate under these conditions. This value was approximately half of the K_M measured for the 1:2 (2.5 ± 0.6 mM) and 1:1 (2.8 ± 0.3 mM) **1**·Cu^{2+}/**2** systems. Interestingly, the V_{max} determined for the 1:2 system (7.3 ± 1.1 × 10^{-7} M s^{-1}) was noticeably higher than both the 1:1 (5.3 ± 0.4 × 10^{-7} M s^{-1}) and 1:3 (5.2 ± 0.3 × 10^{-7} M s^{-1}) **1**·Cu^{2+}/**2** systems, suggesting intrinsic differences exist between the catalytic pockets in the formed assemblies. Re-examination of the catalytic activity at higher concentrations of **HPNPP** (3 mM) showed that the catalytic activity of the 1:2 **1**·Cu^{2+}/**2** system was indeed the highest when working above the K_M (see SI, Figure S4j). The k_{cat} obtained for these three systems were 2.65 ± 0.2 × 10^{-3} s^{-1} (1:1 **1**·Cu^{2+}/**2** system), 3.65 ± 0.6 × 10^{-3} s^{-1} (1:2 **1**·Cu^{2+}/**2**) and 2.60 ± 0.2 ×10^{-3} s^{-1} (1:3 **1**·Cu^{2+}/**2**), which compare well to covalently-linked systems reported by Salvio and Spiccia.[18] For example, our 1:1 **1**·Cu^{2+}/**2** system is 2 times faster than a related 1:1 covalently linked system[18a] and our 1:2 **1**·Cu^{2+}/**2** system is 2 orders of magnitude faster than a related 1:2 covalently-linked system.[18g] The k_{cat} of natural nucleases is in the order of 100 s^{-1}, so there is still room for improvement.[22] These comparisons have been made with the caveat that different reaction conditions are used in each system, but demonstrates that highly efficient catalytic systems can be formed by synergic effects between self-assembled catalytic units.

To demonstrate the dynamic nature of this catalyst system, we performed experiments to modify the ratio of the functional units *in situ*, which enabled up- and down-regulation of catalytic activity. Beginning with a 4:1 **1**·Cu^{2+}/**2** system (where the catalytic activity is low, see Figure 4c), enough C_{16}-guanidinium **2** was added into the reaction medium to give a 1:3 ratio of **1**·Cu^{2+}/**2**, which we have shown possesses much higher catalytic activity.[23] Figure 5b tracks the cleavage of **HPNPP** over time in a 4:1 **1**·Cu^{2+}/**2** mixture (yellow line) and compares it to a system where a 4:1 **1**·Cu^{2+}/**2** system is switched to a 1:3 **1**·Cu^{2+}/**2** system (green line) after 4 minutes. The reaction rate was observed to immediately increase, indicating that the system is able to rapidly reorganize to form a new catalyst system. Figure 5c shows that the reverse is also possible, where a 1:3 **1**·Cu^{2+}/**2** catalyst system is modified *in situ* to form a 4:1 **1**·Cu^{2+}/**2** system, resulting in the down-regulation of catalytic activity (yellow line). The responsiveness of these systems was possible due to the dynamic and modular nature of the self-assembled structures. These results suggest that even more complex systems can be generated in the future by introducing more pre-catalysts containing different functional groups. It also opens up the possibility for the self-selection of a synergistic catalyst from a library of pre-catalysts by use of a transition-state-analogue.[1b,24]

In conclusion, we have demonstrated the formation of a multi-component synergistic catalyst within a dynamic assembly. Such systems offer the ability to modify the ratio of catalytic components to optimize catalytic activity, which is not possible when catalytic units are joined by covalent bonding or immobilized onto solid supports. In the current system, synergism is observed between two different amphiphiles, such that the catalytic activity observed is higher than what is achievable with each of the amphiphiles on its own. Varying the ratio of the two amphiphiles gave rise to catalyst systems possessing different K_M and V_{max} parameters, and suggest key differences exists in the catalytic pockets formed in the different systems. We show that catalyst formation is a highly dynamic process that allows for triggered reorganization and the up- and down-regulation of catalytic activity. Current efforts are aimed at developing this system for the generation of new synergistic catalysts and utilizing the dynamic nature of these systems for the design of stimuli-responsive catalysts in water.

AUTHOR INFORMATION

Corresponding Author

* Jack L.-Y. Chen

orcid.org/0000-0002-4662-4076;
Email: jack.chen@aut.ac.nz

Notes

The authors declare no competing financial interests.

ASSOCIATED CONTENT

Supporting Information

This material is available free of charge via the Internet at http://pubs.acs.org.

Experimental procedures, further detail on experiments described in the manuscript and NMR spectra of novel compounds (PDF).

ACKNOWLEDGMENT

The authors thank Dr Adrian Turner for assistance with TEM imaging and Dr Andrew Whitten for assistance with SANS measurements. This work was supported by a Catalyst: Seeding Grant (CSG-AUT1701), administered by the Royal Society of New Zealand and funded by the Ministry of Business, Innovation and Employment; and by a grant from the Australian Centre for Neutron Scattering, ANSTO (Neutron proposal: 8211). Funding was also received from the MacDiarmid Institute for Advanced Materials and Nanotechnology (Wellington, NZ).

REFERENCES

(1) (a) Hammes, G. G.; Benkovic, S. J.; Hammes-Schiffer, S., Flexibility, Diversity, and Cooperativity: Pillars of Enzyme Catalysis. *Biochemistry* **2011**, *50*, 10422-10430. (b) Sanders, J. K. M., Supramolecular catalysis in transition. *Chem. Eur. J.* **1998**, *4*, 1378-1383. (c) Kirby, A. J., Enzyme mechanisms, models, and mimics. *Angew. Chem. Int. Ed.* **1996**, *35*, 707-724.

(2) (a) Kuah, E.; Toh, S.; Yee, J.; Ma, Q.; Gao, Z. Q., Enzyme Mimics: Advances and Applications. *Chem. Eur. J.* **2016**, *22*, 8404-8430. (b) Raynal, M.; Ballester, P.; Vidal-Ferran, A.; van Leeuwen, P. W. N. M., Supramolecular catalysis. Part 2: artificial enzyme mimics. *Chem. Soc. Rev.* **2014**, *43*, 1734-1787.

(3) (a) Joshi, T.; Graham, B.; Spiccia, L., Macrocyclic Metal Complexes for Metalloenzyme Mimicry and Sensor Development. *Acc. Chem. Res.* **2015**, *48*, 2366-2379. (b) Rebilly, J. N.; Colasson, B.; Bistri, O.; Over, D.; Reinaud, O., Biomimetic cavity-based metal complexes. *Chem. Soc. Rev.* **2015**, *44*, 467-489. (c) Marchetti, L.; Levine, M., Biomimetic Catalysis. *ACS Catal.* **2011**, *1*, 1090-1118.

(4) Wulff, G.; Liu, J. Q., Design of Biomimetic Catalysts by Molecular Imprinting in Synthetic Polymers: The Role of Transition State Stabilization. *Acc. Chem. Res.* **2012**, *45*, 239-247.

(5) (a) Martin, M.; Manea, F.; Fiammengo, R.; Prins, L. J.; Pasquato, L.; Scrimin, P., Metallodendrimers as transphosphorylation catalysts. *J. Am. Chem. Soc.* **2007**, *129*, 6982-6983. (b) Francavilla, C.; Drake, M. D.; Bright, F. V.; Detty, M. R., Dendrimeric organochalcogen catalysts for the activation of hydrogen peroxide: Improved catalytic activity through statistical effects and cooperativity in successive generations. *J. Am. Chem. Soc.* **2001**, *123*, 57-67. (c) Breinbauer, R.; Jacobsen, E. N., Cooperative asymmetric catalysis with dendrimeric [Co(salen)] complexes. *Angew. Chem. Int. Ed.* **2000**, *39*, 3604-3607.

(6) (a) Mancin, F.; Prins, L. J.; Pengo, P.; Pasquato, L.; Tecilla, P.; Scrimin, P., Hydrolytic Metallo-Nanozymes: From Micelles and Vesicles to Gold Nanoparticles. *Molecules* **2016**, *21*, 1014. (b) Savelli, C.; Salvio, R., Guanidine-Based Polymer Brushes Grafted onto Silica Nanoparticles as Efficient Artificial Phosphodiesterases. *Chem. Eur. J.* **2015**, *21*, 5856-5863. (c) Salvio, R.; Cincotti, A., Guanidine based self-assembled monolayers on Au nanoparticles as artificial phosphodiesterases. *RSC Adv.* **2014**, *4*, 28678-28682.

(7) (a) Nagel, Z. D.; Klinman, J. P., A 21(st) century revisionist's view at a turning point in enzymology. *Nat. Chem. Biol.* **2009**, *5*, 543-550. (b) Tokuriki, N.; Tawfik, D. S., Protein Dynamism and Evolvability. *Science* **2009**, *324*, 203-207.

(8) (a) Muñana, P. S.; Ragazzon, G.; Dupont, J.; Ren, C. Z.-J.; Prins, L. J.; Chen, J. L. Y., Substrate-Induced Self-Assembly of Cooperative Catalysts. *Angew. Chem. Int. Ed.* **2018**, *57*, 16469-16474. (b) Ren, C. Z. J.; Munana, P. S.; Dupont, J.; Zhou, S. S.; Chen, J. L. Y., Reversible Formation of a Light-Responsive Catalyst by Utilizing Intermolecular Cooperative Effects. *Angew. Chem. Int. Ed.* **2019**, *58*, 15254-15258.

(9) (a) Afrose, S. P.; Bal, S.; Chatterjee, A.; Das, K.; Das, D., Designed Negative Feedback from Transiently formed Catalytic Nanostructures. *Angew. Chem. Int. Ed.* **2019**, *58*, 15783-15787. (b) Bal, S.; Das, K.; Ahmed, S.; Das, D., Chemically Fueled Dissipative Self-Assembly that Exploits Cooperative Catalysis. *Angew. Chem. Int. Ed.* **2019**, *58*, 244-247. (c) Ma, N. N.; Li, F.; Li, S. Y.; Chu, S. N.; Han, L. L.; Liu, S. D.; Yan, T. F.; Tian, R. Z.; Luo, Q.; Liu, J. Q., A remote optically controlled hydrolase model based on supramolecular assembly and disassembly of its enzyme-like active site. *Nanoscale* **2019**, *11*, 3521-3526. (d) Zozulia, O.; Dolan, M. A.; Korendovych, I. V., Catalytic peptide assemblies. *Chem. Soc. Rev.* **2018**, *47*, 3621-3639. (e) Omosun, T. O.; Hsieh, M. C.; Childers, W. S.; Das, D.; Mehta, A. K.; Anthony, N. R.; Pan, T.; Grover, M. A.; Berland, K. M.; Lynn, D. G., Catalytic diversity in self-propagating peptide assemblies. *Nat. Chem.* **2017**, *9*, 805-809. (f) Zhang, C. Q.; Shafi, R.; Lampel, A.; MacPherson, D.; Pappas, C. G.; Narang, V.; Wang, T.; Maldarelli, C.; Ulijn, R. V., Switchable Hydrolase Based on Reversible Formation of Supramolecular Catalytic Site Using a Self-Assembling Peptide. *Angew. Chem. Int. Ed.* **2017**, *56*, 14511-14515. (g) Singh, N.; Conte, M. P.; Ulijn, R. V.; Miravet, J. F.; Escuder, B., Insight into the esterase like activity demonstrated by an imidazole appended self-assembling hydrogelator. *Chem. Commun.* **2015**, *51*, 13213-13216. (h) Rufo, C. M.; Moroz, Y. S.; Moroz, O. V.; Stohr, J.; Smith, T. A.; Hu, X. Z.; DeGrado, W. F.; Korendovych, I. V., Short peptides self-assemble to produce catalytic amyloids. *Nat. Chem.* **2014**, *6*, 303-309.

(10) (a) De, S.; Klajn, R., Dissipative Self-Assembly Driven by the Consumption of Chemical Fuels. *Adv. Mater.* **2018**, *30*, 1706750. (b) Panettieri, S.; Ulijn, R. V., Energy landscaping in supramolecular materials. *Curr. Opin. Struct. Biol.* **2018**, *51*, 9-18. (c) Merindol, R.; Walther, A., Materials learning from life: concepts for active, adaptive and autonomous molecular systems. *Chem. Soc. Rev.* **2017**, *46*, 5588-5619. (d) van Rossum, S. A. P.; Tena-Solsona, M.; van Esch, J. H.; Eelkema, R.; Boekhoven, J., Dissipative out-of-equilibrium assembly of man-made supramolecular materials. *Chem. Soc. Rev.* **2017**, *46*, 5519-5535. (e) Grzybowski, B. A.; Huck, W. T. S., The nanotechnology of life-inspired systems. *Nat. Nanotechnol.* **2016**, *11*, 584-591.

(11) (a) Ashkenasy, G.; Hermans, T. M.; Otto, S.; Taylor, A. F., Systems chemistry. *Chem. Soc. Rev.* **2017**, *46*, 2543-2554. (b) Miljanic, O. S., Small-Molecule Systems Chemistry. *Chem* **2017**, *2*, 502-524. (c) Mattia, E.; Otto, S., Supramolecular systems chemistry. *Nat. Nanotechnol.* **2015**, *10*, 111-119.

(12) For a related example, see: Fanlo-Virgos, H.; Alba, A. N. R.; Hamieh, S.; Colomb-Delsuc, M.; Otto, S., Transient Substrate-Induced Catalyst Formation in a Dynamic Molecular Network. *Angew. Chem. Int. Ed.* **2014**, *53*, 11346-11350.

(13) (a) Mancin, F.; Scrimin, P.; Tecilla, P., Progress in artificial metallonucleases. *Chem. Commun.* **2012**, *48*, 5545-5559. (b) Lonnberg, H., Cleavage of RNA phosphodiester bonds by small molecular entities: a mechanistic insight. *Org. Biomol. Chem.* **2011**, *9*, 1687-1703.

(14) (a) Zaupa, G.; Mora, C.; Bonomi, R.; Prins, L. J.; Scrimin, P., Catalytic Self-Assembled Monolayers on Au Nanoparticles: The Source of Catalysis of a Transphosphorylation Reaction. *Chem. Eur. J.* **2011**, *17*, 4879-4889. (b) Manea, F.; Houillon, F. B.; Pasquato, L.; Scrimin, P., Nanozymes: Gold-nanoparticle-based transphosphorylation catalysts. *Angew. Chem. Int. Ed.* **2004**, *43*, 6165-6169.

(15) This system was exciting as the catalytic activity could be attributed directly to cooperative effects between catalytically active head groups, and is fundamentally different to conventional micellar catalysis, where rate accelerations are generally attributed to concentration enhancements within the micellar core. For related examples of micellar and vesicular catalysis see (a) Tasca, E.; La Sorella, G.; Sperni, L.; Strukul, G.; Scarso, A., Micellar promoted multi-component synthesis of 1,2,3-triazoles in water at room temperature. *Green Chemistry* **2015**, *17*, 1414-1422. (b) Walde, P.; Umakoshi, H.; Stano, P.; Mavelli, F., Emergent properties arising from the assembly of amphiphiles. Artificial vesicle membranes as reaction promoters and regulators. *Chemical Communications* **2014**, *50*, 10177-10197. (c) Poznik, M.; Konig, B., Cooperative hydrolysis of aryl esters on functionalized membrane surfaces and in micellar solutions. *Org. Biomol. Chem.* **2014**, *12*, 3175-3180. (d) Gruber, B.; Kataev, E.; Aschenbrenner, J.; Stadlbauer, S.; Konig, B., Vesicles and Micelles from Amphiphilic Zinc(II)-Cyclen Complexes as Highly Potent Promoters of Hydrolytic DNA Cleavage. *J. Am. Chem. Soc.* **2011**, *133*, 20704-20707. (e) Dwars, T.; Paetzold, E.; Oehme, G., Reactions in micellar systems. *Angew. Chem. Int. Ed.* **2005**, *44*, 7174-7199. (f) Rispens, T.; Engberts, J. B. F. N., Efficient catalysis of a Diels-Alder reaction by metallo-vesicles in aqueous solution. *Organic Letters* **2001**, *3*, 941-943. (g) Engberts, J. B. F. N., Catalysis by Surfactant Aggregates in Aqueous-Solutions. *Pure and Applied Chemistry* **1992**, *64*, 1653-1660.

(16) (a) Salvio, R.; Volpi, S.; Folcarelli, T.; Casnati, A.; Cacciapaglia, R., A calix[4]arene with acylguanidine units as an efficient catalyst for phosphodiester bond cleavage in RNA and DNA model compounds. *Org. Biomol. Chem.* **2019**, *17*, 7482-7492. (b) Salvio, R., The Guanidinium Unit in the Catalysis of Phosphoryl Transfer Reactions: From Molecular Spacers to Nanostructured Supports. *Chem. Eur. J.* **2015**, *21*, 10960-10971. (c) Salvio, R.; Cacciapaglia, R.; Mandolini, L.; Sansone, F.; Casnati, A., Diguanidinocalix[4]arenes as effective and selective catalysts of the cleavage of diribonucleoside monophosphates. *RSC Adv.* **2014**, *4*, 34412-34416. (d) Salvio, R.; Mandolini, L.; Savelli, C., Guanidine-Guanidinium Cooperation in Bifunctional Artificial Phosphodiesterases Based on Diphenylmethane Spacers; gem-Dialkyl Effect on Catalytic Efficiency. *J. Org. Chem.* **2013**, *78*, 7259-7263. (e) Baldini, L.; Cacciapaglia, R.; Casnati, A.; Mandolini, L.; Salvio, R.; Sansone, F.; Ungaro, R., Upper Rim Guanidinocalix[4]arenes as Artificial Phosphodiesterases. *J. Org. Chem.* **2012**, *77*, 3381-3389. (f) Perreault, D. M.; Cabell, L. A.; Anslyn, E. V., Using guanidinium groups for the recognition of RNA and as catalysts for the hydrolysis of RNA. *Bioorg. Med. Chem.* **1997**, *5*, 1209-1220.

(17) (a) Blondeau, P.; Segura, M.; Perez-Fernandez, R.; de Mendoza, J., Molecular recognition of oxoanions based on guanidinium receptors. *Chem. Soc. Rev.* **2007**, *36*, 198-210. (b) Schug, K. A.; Lindner, W., Noncovalent binding between guanidinium and anionic groups: Focus on biological- and synthetic-based arginine/guanidinium interactions with phosph[on]ate and sulf[on]ate residues. *Chem. Rev.* **2005**, *105*, 67-113.

(18) (a) Salvio, R.; Volpi, S.; Cacciapaglia, R.; Sansone, F.; Mandolini, L.; Casnati, A., Upper Rim Bifunctional cone-Calix[4]arenes Based on a Ligated Metal Ion and a Guanidinium Unit as DNAase and RNAase Mimics. *J. Org. Chem.* **2016**, *81*, 4728-4735. (b) Tjioe, L.; Joshi, T.; Graham, B.; Spiccia, L., Synthesis and phosphate ester cleavage properties of copper(II) complexes of guanidinium-bridged bis(1,4,7-triazacyclononane) ligands. *Polyhedron* **2016**, *120*, 11-17. (c) Zhang, X. P.; Liu, X. P.; Phillips, D. L.; Zhao, C. Y., Hydrolysis mechanisms of BNPP mediated by facial copper(II) complexes bearing single alkyl guanidine pendants: cooperation between the metal centers and the guanidine pendants. *Dalton Trans.* **2016**, *45*, 1593-1603. (d) Salvio, R.; Volpi, S.; Cacciapaglia, R.; Casnati, A.; Mandolini, L.; Sansone, F.,

Ribonuclease Activity of an Artificial Catalyst That Combines a Ligated Cu-II Ion and a Guanidinium Group at the Upper Rim of a cone-Calix[4]arene Platform. *J. Org. Chem.* **2015**, *80*, 5887-5893. (e) Tjioe, L.; Joshi, T.; Forsyth, C. M.; Moubaraki, B.; Murray, K. S.; Brugger, J.; Graham, B.; Spiccia, L., Phosphodiester Cleavage Properties of Copper(II) Complexes of 1,4,7-Triazacyclononane Ligands Bearing Single Alkyl Guanidine Pendants. *Inorg. Chem.* **2012**, *51*, 939-953. (f) Tjioe, L.; Meininger, A.; Joshi, T.; Spiccia, L.; Graham, B., Efficient Plasmid DNA Cleavage by Copper(II) Complexes of 1,4,7-Triazacyclononane Ligands Featuring Xylyl-Linked Guanidinium Groups. *Inorg. Chem.* **2011**, *50*, 4327-4339. (g) Tjioe, L.; Joshi, T.; Brugger, J.; Graham, B.; Spiccia, L., Synthesis, Structure, and DNA Cleavage Properties of Copper(II) Complexes of 1,4,7-Triazacyclononane Ligands Featuring Pairs of Guanidine Pendants. *Inorg. Chem.* **2011**, *50*, 621-635. (h) Salvio, R.; Cacciapaglia, R.; Mandolini, L., General Base-Guanidinium Cooperation in Bifunctional Artificial Phosphodiesterases. *J. Org. Chem.* **2011**, *76*, 5438-5443. (i) Ait-Haddou, H.; Sumaoka, J.; Wiskur, S. L.; Folmer-Andersen, J. F.; Anslyn, E. V., Remarkable cooperativity between a Zn-II ion and guanidinium/ammonium groups in the hydrolysis of RNA. *Angew. Chem. Int. Ed.* **2002**, *41*, 4014-4016.

(19) A higher concentration was used to allow comparison to subsequent experiments performed in 20% DMSO/water, where the system has a higher CAC due to the decreased polarity of the solvent mixture.

(20) (a) Kneeland, D. M.; Ariga, K.; Lynch, V. M.; Huang, C. Y.; Anslyn, E. V., Bis(Alkylguanidinium) Receptors for Phosphodiesters - Effect of Counterions, Solvent Mixtures, and Cavity Flexibility on Complexation. *J. Am. Chem. Soc.* **1993**, *115*, 10042-10055. (b) Ariga, K.; Anslyn, E. V., Manipulating the Stoichiometry and Strength of Phosphodiester Binding to a Bisguanidine Cleft in Dmso Water Solutions. *J. Org. Chem.* **1992**, *57*, 417-420.

(21) (a) Corona-Martinez, D. O.; Taran, O.; Yatsimirsky, A. K., Mechanism of general acid-base catalysis in transesterification of an RNA model phosphodiester studied with strongly basic catalysts. *Org. Biomol. Chem.* **2010**, *8*, 873-880. (b) Sanchez-Lombardo, I.; Yatsimirsky, A. K., Simplified speciation and improved phosphodiesterolytic activity of hydroxo complexes of trivalent lanthanides in aqueous DMSO. *Inorg. Chem.* **2008**, *47*, 2514-2525.

(22) Serpersu, E. H.; Shortle, D.; Mildvan, A. S. Kinetic and magnetic resonance studies of active-site mutants of Staphylococcal nuclease: factors contributing to catalysis. *Biochemistry* **1987**, *26*, 1289-1300.

(23) Additional reaction components were also added to the reaction medium to maintain the concentrations of all other species constant.

(24) Brisig, B.; Sanders, J. K. M.; Otto, S., Selection and amplification of a catalyst from a dynamic combinatorial library. *Angew. Chem. Int. Ed.* **2003**, *42*, 1270-1273.

SYNOPSIS TOC.

Cooperativity between functional groups in a self-assembled system allows for the easy generation of numerous catalyst systems. Such systems are highly dynamic, allowing for triggered re-organization and the up- and down-regulation of catalytic activity.

TOC graphic